International Journal of Medicine and Pharmaceutical Sciences (IJMPS)
ISSN(P): 2250-0049; ISSN(E): 2321-0095
Vol. 5, Issue 4, Aug 2015, 91-104

STIMULATING THE DNA FRAGMENTS THROUGH HIGHLY EFFECTIVE CU(II), CO(II), NI(II) AND MN(II) SCHIFF BASE METAL COMPLEXES – AN *IN VITRO* APPROACH OF ANTIOXIDANT AND ANTIBIOGRAM ASSAY

RAJU ASHOKAN & RANGAPPAN RAJAVEL

Department of Chemistry, Periyar University, Salem, Tamil Nadu, India

ABSTRACT

With the aim of exploring the biological properties of coordination compounds, we report for the first time the synthesis of precursors 4-[(2-Amino-phenylimino)-methyl]-benzene-1, 3-diol, *N*-(4-Methoxy-benzylidene)-benzene-1, 2-diamine and its Cu(II), Co(II), Ni(II), Mn(II) complexes derived from condensation route of 2,4-dihydroxybenzaldehyde, o-phenylenediammine and anisaldehyde were characterized by a set of chemical and spectroscopic measurements using elemental analysis, electrical conductance, magnetic susceptibility and spectral techniques (IR, UV–Vis, ^{1}H NMR and EPR). Elemental data are consistent with the proposed formula. IR spectra confirm the bidentate and tetradentate nature of the Schiff base ligands and coordination of metal complexes with the ligands. The distorted octahedral geometry around Cu(II), Co(II), Ni(II), and Mn(II) complexes were suggested by UV–Vis spectra and magnetic moment data. Absorption titration, electrochemical analyses and viscosity measurements have also been carried out to determine the mode of binding. Interaction of metal complexes with DNA revealed an intercalative mode of binding between them. The cleavage products of the complexes analyzed by neutral agarose gel electrophoresis indicated that the interaction of the metal complexes with supercoiled plasmid DNA yielded linear, nicked or degraded DNA. Antimicrobial studies showed an effective antimicrobial activity of the metal complexes after coordination with the ligands.

KEYWORDS: DNA Binding, Nucleolytic Cleavage, Antibiogram Assay, Scavenging Effect

INTRODUCTION

Coordination chemistry is a fascinating branch in inorganic chemistry, and the beauty lies in the fact that minute changes in the metal ion environment induce dramatic changes in properties of compounds. Studies on transition metal complexes have achieved great interest due to their versatile applications in different areas such as catalysis, bioinorganic, biomimetic and medicinal chemistry. Nowadays coordination chemistry comprises a major portion of current inorganic research. It also provides many directions in research such as, in molecular magnetism, supramolecular chemistry, non-silicon based devices, precursors for vapour phase deposition, single molecules based photonic devices and sensors [1]. Diverse coordination compounds arising from interesting ligand systems containing different donor sites. The nitrogen-oxygen donor ligands, possess a special place due to their wide spread applications and interesting coordination capability with transition metal ions [2-4]. Based on above facts, our research has focussed to synthesize novel Schiff base complexes as new therapeutic and diagnostic agents in medicinal fields. To best of our knowledge, no work has been reported on the condensed reaction of the 2, 4-dihydroxybenzaldehyde, o-phenylenediammine and anisaldehyde and its transition metal complexes as chemical nucleases.

EXPERIMENTAL

Materials

All the chemicals and solvents used for synthesis were of commercially available reagent grade. 2, 4-dihydroxybenzaldehyde, o-phenylenediammine and anisaldehyde are purchased from Sigma–Aldrich and Loba chemicals. All the metal (II) complexes are used as metal acetates [Cu(II), Co(II), Ni(II) and Mn(II)]. Ethanol, DMSO and DMF are used as solvent were purchased from Merck and Loba chemicals.

Analysis and Physical Measurements

The elemental analyses (C, H and N) were performed by using Vario EL III CHN analyser at STIC, Cochin University of Science and Technology, Kerala, India. Molar conductance values are measured for freshly prepared solution of metal complexes in DMF by using an ELICO CM 185 conductivity Bridge. IR spectra were recorded in KBr pellets by using Thermo Nicolet, Avatar 370 model spectrophotometer (4000-400 cm^{-1}). The electronic spectra for synthesized compounds were analysed by using Perkin Elmer Lambda-25 spectrophotometer (200-800nm). Magnetic susceptibility measurements of the chelates were measured by using Gouy balance. The ^1H NMR spectra were recorded in DMSO-d_6 on a BRUKER ADVANCED III 400 MHz spectrophotometer using TMS as an internal reference. EPR spectra were recorded on E-112 ESR spectrometer at X-band microwave frequencies for powdered samples.

Synthesis of Precursor 4-[(2-Amino-Phenylimino)-Methyl]-Benzene-1, 3-Diol

An ethanolic solution (10 mL) of 2, 4-dihydroxybenzaldehyde (0.138 g, 1 mmole) was added to an ethanolic solution (10 mL) containing o-phenylenediammine (0.108 g, 1 mmole). The mixture was stirred for an hour [6]. The reaction mixture was cooled at room temperature and the solid compound was filtered. Yield: 65 %, Colour: lemonish yellow, M.p.= 68-69 °C, IR (KBr discs): 3395 ν(NH_2); 1615 ν(-CH=N) ; 1566 ν(C=C); 3382 ν(-OH). H^1 NMR (DMSO-d_6, δ ppm): 7.55-7.63 ppm (m, Ar-H), 8.68 ppm (s, NH), 8.21 ppm (s, CH=N), 10.11 ppm (Ph-OH), UV–Vis [λ_{max}(nm)]: 283 (π→ π*), 36 (n→ π*).

Synthesis of Precursor *N*-(4-Methoxy-Benzylidene)-Benzene-1, 2-Diamine

An ethanolic solution (10 mL) of o-phenylenediammine (0.108 g, 1 mmole) was added to an ethanolic solution (10 mL) containing anisaldehyde (0.136 g, 1 mmole). The mixture was stirred for an hour. The reaction was cooled at room temperature and the solid compound was filtered. Yield: 72 %, Colour: pale yellow, M.p.= 76-78 °C, IR (KBr discs): 3392 ν(NH_2); 1612 ν(-CH=N) ; 1560 ν(C=C); 3368 ν(-OH). H^1 NMR (DMSO-d_6, δ ppm): 7.62-7.98 ppm (m, Ar-H), 8.72 ppm (s, NH), 8.28 ppm (s, CH=N), 9.92 ppm (Ph-OH), UV–Vis [λ_{max}(nm)]: 263 (π→ π*), 380 (n→ π*).

Synthesis of Schiff Bases

L^1: 4-[(2-Amino-phenylimino)-methyl]-benzene-1, 3-diol (1 mmole) in 10 mL of ethanol, o-phenylenediammine (1 mmole) in 10 mL of ethanol were mixed and heated at reflux for 2 hrs as shown in Figure 1. The resulting yellow color solution was allowed to cool. The dark yellow color product was obtained and dried. Yield: 74 %. M.p: 155-156 °C. *Anal. Calc. For* $C_{20}H_{16}N_2O_4$: C, 68.96; H, 4.59; N, 8.04. Found: C, 68.95; H, 4.59; N, 8.03 (%). IR (KBr pellet, cm^{-1}): 3385 ν(-OH); 1616 ν(-CH=N) ; 1293 (-C-O). UV–Vis λ_{max} (nm), 312, 368 (π→ π*, n→ π*).H^1 NMR (DMSO-d_6, δ ppm): 6.6-7.4 ppm (m, Ar-H), 8.12 ppm (s, CH=N), 10.3 ppm (Ph-OH).

L^2: *N*-(4-Methoxy-benzylidene)-benzene-1, 2-diamine (1 mmole) in 10 mL of ethanol, anisaldehyde (1 mmole) in 10 mL of ethanol were mixed and heated at reflux for 2 hrs. The resulting yellow color solution was allowed to cool. The pale yellow color product was obtained and dried. Yield: 68 %. M.p: 148-150 °C. *Anal. Calc. For* $C_{22}H_{20}N_2O_2$: C, 76.74; H, 5.81; N, 8.13. Found: C, 76.73; H, 5.80; N, 8.12 (%). IR (KBr pellet, cm^{-1}): 1612 ν(-CH=N) ; 1275 ν(-C-O). UV–Vis λ_{max} (nm), 315, 370 (π→ π*, n→ π*). H^1 NMR (DMSO-d_6, δ ppm): 7.12-8.23 ppm (m, Ar-H), 8.23 ppm (s, CH=N), 9.22 ppm (s, Ph-OH).

General Procedure for the Synthesis of Metal Complexes

An ethanolic solution (20 mL) containing L^1 (0.348 g, 1 mmole) and L^2 (0.344 g, 1 mmole) were added to a solution of Metal(II) acetates of Cu(II), Co(II), Ni(II) and Mn(II) (1 mmole) in 20 ml of ethanol. The solution was refluxed for 3 hrs as shown in Figure 1 and then allowed to stand at room temperature for 24 hrs [7]. The resulting powder was filtered and dried in vacuum.

Synthesis of Cu ($C_{42}H_{34}N_4O_6$)

Yield: 62 %. M.p: 220-221 °C. *Anal. Calc. For* Cu($C_{42}H_{34}N_4O_6$): C, 66.84; H, 4.50; N, 7.42; Cu, 8.42. Found: C, 66.83; H, 4.50; N, 7.42; Cu, 8.41 (%). IR (KBr pellet, cm^{-1}): 1608 ν(-CH=N) ; 1292 ν(-C-O) ; 489 ν(-M-N) ; 537 ν(-M-O). UV–Vis λ_{max} (nm), 290, 365, 440 (π→ π*, n→ π*, L→MCT); 520, 575, 625 (d→d). μ_{eff} (BM): 1.74.

Synthesis of Ni ($C_{42}H_{34}N_4O_6$)

Yield: 65 %. M.p: 222–224 °C. *Anal. Calc. For* Ni($C_{42}H_{34}N_4O_6$): C, 67.28; H, 4.53; N, 7.47; Ni, 7.83. Found: C, 67.27; H, 4.52; N, 7.46; Ni, 7.83 (%). IR (KBr pellet, cm^{-1}): 1607 ν(-CH=N) ; 1297 ν(-C-O) ; 458 ν(-M-N) ; 543 ν(-M-O). UV–Vis λ_{max} (nm), 275, 370, 455 (π→ π*, n→ π*, L→MCT); 513,555, 618 (d→d). μ_{eff} (BM): 3.17.

Synthesis of Co ($C_{42}H_{34}N_4O_6$)

Yield: 61 %. M.p: 230-233 °C. *Anal. Calc. For* Co($C_{42}H_{34}N_4O_6$): C, 67.65; H, 4.50; N, 7.51; Co, 7.90. Found: C, 67.64; H, 4.49; N, 7.50; Co, 7.90 (%). IR (KBr pellet, cm^{-1}): 1610 ν(-CH=N) ; 1294 ν(-C-O) ; 451 ν(-M-N) ; 518 ν(-M-O). UV–Vis λ_{max} (nm), 280, 390, 470 (π→ π*, n→ π*, L→MCT); 528,562, 620 (d→d). μ_{eff} (BM): 4.86.

Synthesis of Mn ($C_{42}H_{34}N_4O_6$)

Yield: 67 %. M.p: 215-216 °C. *Anal. Calc. For* Mn($C_{42}H_{34}N_4O_6$): C, 67.64; H, 4.51; N, 7.50; Mn, 7.90. Found: C, 67.64; H, 4.49; N, 7.50; Mn, 7.35 (%). IR (KBr pellet, cm^{-1}): 1606 ν(-CH=N) ; 1289 ν(-C-O) ; 468 ν(-M-N) ; 566 ν(-M-O). UV–Vis λ_{max} (nm), 260, 375, 475 (π→ π*, n→ π*, L→MCT); 602 (d→d). μ_{eff} (BM): 5.81.

Pharmacology

Evaluation of Antimicrobial Activity

The antibacterial and antifungal activity of Schiff base ligands and their metal complexes [Cu(II), Co(II), Ni(II) and Mn(II)] in DMF solvent were screened against some microorganisms by disc diffusion method. The pathogenic bacteria and fungi involved in present investigation include are *Staphylococcus aureus*, *Bacillus subtilis*, *Escherichia coli*, *Klebsilla pneumonia* and the fungi are *Fusarium oxysporum* and *Aspergillus fumigates*. The antibiotic *Streptomycin* and *Clotrimazole* was used as control for anti-bacterial and anti-fungal activity. All compounds were dissolved in DMF solvent to obtain concentration of 100 µg/ mL. The test was performed on medium potato dextrose agar contains infusion of 200 g

potatoes, 6 g dextrose and 15 g agar. Uniform size filter paper discs (three disks per compound) were impregnated by equal volume from the specific concentration of dissolved tested compounds and carefully placed on incubated agar surface. The bacteria were incubated for 36 hrs at 27 °C and fungi for 48 hrs at 24 °C. The activity was calculated on the basis of the size of inhibition zone formed around paper disc on seeded plates [8-10].

Nucleic Acid Separation by Agarose Gel Electrophoresis

Agarose gel electrophoresis method was employed for cleavage activity. The DNA (pBR322 plasmid) was cultured, isolated and experiments were performed. The tested samples contains 50 μM pBR322 DNA, 50 μM metal complexes and 50 μM H_2O_2 in tris-HCl buffer (pH 7.2) are incubated at 37 °C for 2 hrs. The samples were electrophoresed for 2 hrs at 50 V on 1% agarose gel using tris-acetic acid-EDTA buffer (pH 7.2). Using 1 μg cm^{-3} ethidium bromide (EB), the gel was stained and photographed under ultraviolet light at 360 nm. All the experiments were performed at room temperature [11-13].

Dna Binding Experiments

Electronic Absorption Titration

Electronic absorption spectroscopy has been widely employed to determine the binding characteristics of metal complexes with DNA [14]. The DNA experiments performed in 5 mM Tris–HCl/ 50 mM NaCl in water at pH 7.0, using DMF solution of metal complexes. The concentration of CT DNA was determined per nucleotide by taking the absorption coefficient (6600 mol^{-1} cm^{-1}) at 260 nm. The absorbance was recorded after successive addition of CT-DNA, while measuring the absorption spectrum an equal amount of CT DNA was added to both the compound solution and the reference solution to eliminate the absorbance of CT DNA itself.

Viscosity Measurements

Viscosity experiments were conducted on an Ostwald viscometer, immersed in a thermostat water-bath maintained at a constant temperature at 30.0±0.1 °C. CT DNA samples of approximately 0.5 mM were prepared by sonicating in order minimize complexities arising from CT DNA flexibility. Each sample was measured in triplicate and the average flow time was calculated with a digital. Data were presented as $(\eta/\eta o)^{1/3}$ versus the ratio of concentration of the compound and DNA, where η is the viscosity of CT DNA solution in the presence of complex, and ηo is the viscosity of CT DNA solution in the absence of complex. Viscosity values were calculated after correcting the flow time of buffer alone (t_0), $\eta = (t-t_0)/t_0$.

Cyclic Voltammetry in DNA Binding Studies

Cyclic voltammetry studies were performed on a CHI 760 electrochemical analyzer with three electrode system of glassy carbon as the working electrode, a platinum wire as auxiliary electrode and Ag/AgCl as the reference electrode.

RESULTS AND DISCUSSIONS

Chemistry

All the complexes [Cu(II), Co(II), Ni(II) and Mn(II)] were coloured, stable at room temperature and non-hygroscopic in nature. These complexes are completely soluble in DMF and DMSO whereas insoluble in water and many organic solvents. The analytical data showed that the complexes had stoichiometry of the type ML_1L_2 [M = Cu(II), Co(II), Ni(II) and Mn(II)] respectively, where L_1 and L_2 are Schiff base ligands. The observed molar conductance values for

complexes are too low (11.83–14.30 $ohm^{-1}cm^2\ mol^{-1}$) which indicates the non-electrolytic nature.

ESR Spectrum of the Cu (II) Complex

Electron paramagnetic resonance is a powerful experimental technique allowing extracting details of the electronic structure of complexes with unpaired electrons. EPR can be used to map the distribution of an unpaired electron in a molecule and, thus obtain information to which extent the electrons are delocalized over the ligands.

The EPR spectra of $Cu(C_{42}H_{34}N_4O_6)$ complex recorded at liquid nitrogen temperature. From these spectra, g|| and $g_\perp$ values have been evaluated and were found to be 2.28 and 2.06 respectively. The g|| values are greater than the corresponding $g_\perp$ values than free electron spin (2.0027) and therefore the complexes should have unpaired electron in its $d_{x^2-y^2}$ molecular orbital [15-16]. It is reported that g|| is a moderately sensitive function for indicating covalence, for a covalent environment g|| is normally <2.3 and for ionic environment it should be >2.3. In the present case, the g|| values are <2.3, which indicates covalent environment in the complexes. This suggests that these mononuclear copper(II) complex have appreciable covalent character in bonding involving the metal ion and ligand. According to Hathaway and Billing, in an axial symmetry, the g-values are related by $G = (g\| - 2.0027)/ (g\perp - 2.0027) = 4.0$, if G > 4, the exchange interaction between copper(II) centers in the solid state is negligible. Whereas G < 4, a considerable exchange interaction occurs in the solid state complexes. The G value of complexes are 4.66 respectively, for $Cu(C_{42}H_{34}N_4O_6)$ complex, ruling out the exchange interactions. Thus, the results suggest that Cu(II) complex possesses distorted octahedral geometry.

The molecular–orbital coefficient parameters, α^2, a measure of the covalency of the in-plane σ -bonding between the 3d and ligand orbitals and β^2, the covalency of the in-plane π-bonding, were calculated employing the equations,

$$\alpha^2 = -(A_\| /0.036) + (g_\| - 2.0027) + 3/7\ (g_\perp - 2.0027) + 0.04$$

$$\beta^2 = (g_\| - 2.0027)\ E/ -8\lambda\alpha^2$$

Where k = -828 cm^{-1} for free Cu(II) and E is the electronic transition energy. The α^2 and β^2 values are 0.541 and 0.559, respectively. The lower value of α^2 compared to β^2 indicates σ-bonding in-plane is more covalent than in-plane π-bonding. These data are in agreement with the proposed geometry [17].

Molecular Modelling

The modern foremost advances in the computational chemistry tools provides an alternative, approximate, approach for obtaining the 3D dimensional structures of the complexes in the case of absence of X-ray crystal structure.

The optimized geometry of the $Cu(C_{42}H_{34}N_4O_6)$ complex is represented with some of selected structural parameters (bond length and bond angles). This molecular modelling structure also shows the stereochemistry of the complex. Based on the proposed structure (Figure 3), the 3D molecular modeling of CuL_1L_2 was carried out with the CS Chem 3D Ultra Molecular Modeling and Analysis Program. According to these parameters we could determine Schiff base metal complex forms octahedral environment around the Cu atoms, respectively.

Antimicrobial Results

Antibacterial

In case of bacteriological studies, the results were compared with the standard drug *Streptomycine*. It was observed that, $Cu(C_{42}H_{34}N_4O_6)$ complex was found potentially active against all bacterial strains. The $Cu(C_{42}H_{34}N_4O_6)$

complex exhibit better antibacterial activity than their SB- ligands $C_{20}H_{16}N_2O_4$, $C_{22}H_{20}N_2O_2$ and its Co($C_{42}H_{34}N_4O_6$), Ni($C_{42}H_{34}N_4O_6$), Mn($C_{42}H_{34}N_4O_6$) against all the four bacteria. It was evident that, overall potency of the uncoordinated compounds was enhanced on coordination with metal ions [18].

Antifungal

In case of antifungal activity, the results were compared with the standard drug *Clotrimazole*. All Schiff bases were show high activity against fungal species. Co($C_{42}H_{34}N_4O_6$) complex showed significantly enhanced antifungal activity than their SB- ligands $C_{20}H_{16}N_2O_4$, $C_{22}H_{20}N_2O_2$ and its Cu($C_{42}H_{34}N_4O_6$), Ni($C_{42}H_{34}N_4O_6$), Mn($C_{42}H_{34}N_4O_6$). The metal complexes of the Schiff base showed much enhanced activity as compared to the uncoordinated compounds. It was evident from the data that, this activity significantly increased on coordination [19]. The studies showed that the newly synthesized compounds possess higher antifungal activity than the antibacterial property.

DNA Cleavage Study by Gel Electrophoresis

After binding to DNA, the synthesized metal complexes can induce several changes in the DNA conformation, such as bending, intercalation, micro loop formation and subsequent DNA shorting lead to decrease in molecular weight of DNA**.** In the presence of H_2O_2, supercoiled pBR322 DNA cleavage ability of complexes was determined by agarose gel electrophoresis method. All the complexes show considerable DNA cleavage ability. When circular plasmid DNA is subjected to electrophoresis, migration will be observed in supercoil form (Form I). If scission occurs on one strand (nicking), the supercoil will relax to form a slower moving open circular form (Form II). If both strands are cleaved, a linear form (Form III) will be formed and it migrates between Forms-I and -II. Figure 4 shows the gel electrophoretic results of complexes interaction with pBR322 DNA. The DNA cleavage efficiency of the complexes was due to the different binding affinity of the complex to DNA [20-23]. Control experiment did not show any apparent cleavage of DNA alone (lane 1& 2). Cu($C_{42}H_{34}N_4O_6$), Ni($C_{42}H_{34}N_4O_6$), Co($C_{42}H_{34}N_4O_6$), Mn($C_{42}H_{34}N_4O_6$) complexes in the presence of H_2O_2 (lanes 3, 4, 5 & 6) at higher concentration (50 μM) show cleavage activity which results in conversion of supercoiled DNA (Form-I) to open circular form (Form-II). These observations show the presence of diffusible radical species in the nuclease mechanism. This can be observed by quenching of DNA cleavage in the presence of DMF, suggesting the possibility of the formation of HO° radicals as the reactive species. For instance, generation of a HO° radical adduct by the copper(II)–H_2O_2 system resembles the Fenton reaction (Fe^{2+}–H_2O_2) [24]. In the presence of H_2O_2, Cu^{2+} ion get oxidized and generate the HO° radicals as follows:

$$(Cu^{2+} + H_2O_2 \rightarrow Cu^{+} + HO^{\circ} + H^{+})$$

These highly reactive hydroxyl radical species can cleave the DNA by abstraction of the hydrogen atom from the deoxyribose sugar. The cleavage activity may be due to the intercalative interaction of the complexes with the DNA strands in the presence of H_2O_2 induces oxidative DNA cleavage. From the observed results, it is concluded that all the synthesized Schiff base Cu($C_{42}H_{34}N_4O_6$), Ni($C_{42}H_{34}N_4O_6$), Co($C_{42}H_{34}N_4O_6$), Mn($C_{42}H_{34}N_4O_6$) complexes effectively cleaves DNA.

Absorption Spectral Characteristics of DNA Binding

The results of absorption spectra of the compounds in the absence and presence of CT-DNA are given in Figure 5. Upon increasing the concentration of DNA to the test compounds, the absorption bands of the complexes Cu($C_{42}H_{34}N_4O_6$)

at 355 nm and $Co(C_{42}H_{34}N_4O_6)$ at 367 nm exhibited a hypochromism of about 8.54% and 3.72% with red shifts of 3 and 2 nm, respectively. These results suggested an intimate association of compounds with CT-DNA and confirm the mode of binding through intercalation. After intercalation, the π* orbital of the intercalated compounds could couple with π orbitals of the base pairs, thus decreasing the π→ π* transition energies, hence resulting in hypochromism [24].

From the absorption data, the intrinsic binding constant (K_b) (Figure 6) was determined from the plot of [DNA]/(ε_a-ε_f) versus [DNA] using the following equation:

$$[DNA]/(\varepsilon_a-\varepsilon_f) = [DNA]/(\varepsilon_b-\varepsilon_f)+ [K_b(\varepsilon_b-\varepsilon_f)]^{-1}$$

where [DNA] is the concentration of CT DNA in base pairs. The apparent absorption coefficients ε_a, ε_f and ε_b correspond to A_{obs}./ [M], the extinction coefficient for the metal(II) complex in the fully bound form, respectively [25]. K_b is given by the ratio of slope to the intercept. The magnitudes of intrinsic binding constants (K_b) were calculated to be 6.3(±0.10) x 10^4 M^{-1} and 2.6(±0.16) x 10^4 M^{-1} for $Cu(C_{42}H_{34}N_4O_6)$ and $Co(C_{42}H_{34}N_4O_6)$ complexes respectively.

Viscosity Measurements

The viscosity measurements of CT-DNA are regarded as the least ambiguous and the most critical tests of a binding model in solution in the absence of crystallographic structural data. Due to its sensitivity to the change of length of DNA, viscosity determination may be the most effective means to study the binding mode of complexes to DNA [26]. Measuring the viscosity of DNA is a classical technique used to analyze the DNA binding mode in solution. Under appropriate conditions, intercalation of drugs, such as ethidium bromide [EB], causes a significant increase in the viscosity of a DNA solution due to the increase in the separation of the base pairs of the intercalation sites and hence, results in an increase in the overall DNA contour length, as shown in Figure 7. The viscosity of the DNA solution increased when ratio of synthesized Schiff base $Cu(C_{42}H_{34}N_4O_6)$, $Ni(C_{42}H_{34}N_4O_6)$, $Co(C_{42}H_{34}N_4O_6)$, $Mn(C_{42}H_{34}N_4O_6)$ complexes increased. Due to strong intercalation, the DNA-intercalator EB increases the relative viscosity of DNA. Complexes exhibit minor increase in the relative viscosity of CT-DNA when compared to EB, suggests an intercalation mode between the complexes and DNA.. The increase in viscosity of DNA is ascribed to the intercalative binding mode of the drug because this could cause the effective length of the DNA to increase [27].

ELECTROCHEMICAL STUDY OF DNA BINDING OF COMPLEXES

In Reduction: In the absence and presence of CT DNA [28-29], the reduction cathodic peak appears at **Free**: $E_{1/2}$ (V)= -1.31, ΔEp(mV) = 220.: **Bound:** $E_{1/2}$ (V)= -1.18, ΔEp(mV) = 80, for $Cu(C_{42}H_{34}N_4O_6)$ complex. This indicates that the reaction of the complex on the glassy carbon electrode surface is quasi-reversible redox process. The incremental addition of CT DNA to the complex causes a negative shift in $E_{1/2}$ (V) of 13 V, and a decrease in ΔEp of 140 mV.

In Oxidation: In the absence of CT DNA [30], first redox couple anodic peak appears at **Free**: $E_{1/2}$ (V)= 0.70, ΔEp(mV) = 130.: **Bound:** $E^1_{1/2}$ (V)= 0.66, ΔE^1p(mV) = 120. This indicates that the reaction of the complex on the glassy carbon electrode surface is quasi-reversible redox process. The addition of CT DNA to the complex the redox couples cause a negative shift in $E_{1/2}$ and a decrease in ΔEp. The results show that $Cu(C_{42}H_{34}N_4O_6)$ complex stabilizes the duplex (GC pairs) and binds with DNA.

CONCLUSIONS

In this work, a systematic approach to the synthesis of mononuclear metal(II) complexes containing 2,4-dihydroxybenzaldehyde, o-phenylenediammine and anisaldehyde were carried out and, were characterized by various spectroscopic techniques. The IR, electronic transition and g tensor data lead to the conclusion that the central metal ion assumes a distorted octahedral geometry. We have evaluated *in vitro* antibacterial and antifungal activities of newly synthesized Schiff base ligands and their metal complexes. The Cu($C_{42}H_{34}N_4O_6$) complex has higher potency against Gram-positive bacteria than Gram-negative bacteria. Copper may easily interact with radicals, especially with molecular oxygen. The DNA binding ability of the complexes were assessed by absorption spectroscopy, viscosity measurement and cyclic voltammetry studies which inferred an intercalative mode of binding with binding constants range of 10^4 M^{-1}. The DNA cleavage capabilities of complexes in the presence of H_2O_2 revealed their potential nuclease activity to cleave pBR322 DNA. These findings clearly indicate that the complexes may have potential practical applications. Results obtained from our presented work would be useful to understand the mechanism of interactions of the small molecule compound binding to DNA and helpful in the development of their potential biological, pharmaceutical and physiological implications in the future.

ACKNOWLEDGEMENTS

The author is indebted to Supervisor for his encouragement and support. STIC Cochin and Progen lab are gratefully acknowledged for providing instrumental facilities.

REFERENCES

1. A.B.P. Lever, comprehensive coordination chemistry (II) 1987.
2. F.H.Case, A.A. Schilt, N.Simonzadeh, Anal.chem. 56 (1984) 2860-2862
3. M.R. Maurya, S. Agarwal, M.Abid, A.Azam, C.Bader, M.Ebel, D.Rehder, Dalton Trans, (2006) 937-947.
4. R.C. Maurya, S.Rajput, J.Mol.Struct. 833 (2007) 133-144.
5. E. Akila, M. Usharani, S. Ramachandran, P. Jayaseelan, G. Velraj, R. Rajavel, Arabian. J. Chem, http://dx.doi.org/10.1016/j.arabjc.2013.11.031.
6. Madappa B. Halli , R.B. Sumathi, J. Mol. Struct. 1022 (2012) 130.
7. Mohammad Akbar Ali, Aminul Huq Mirza, Trans. Met. Chem. 27 (2002) 268.
8. P. Kavitha, M. Saritha, K. Laxma Reddy, Spectrochim. Acta Part A. 102 (2013) 159.
9. Huilu Wu, Jingkun Yuan, Ying Bai, Hua Wang, Guolong Pan, Jin Kong, J. Photochem. Photobiol. 116 (2012) 13.
10. Charikleia Tolia , Athanassios N. Papadopoulos , Catherine P. Raptopoulou , Vassilis Psycharis , Claudio Garino , Luca Salassa , George Psomas, J. Inorg. Biochem. 123 (2013) 53.
11. S.R. Kanatt, R. Chander, A. Sharma, Food Chem. 106 (2008) 521.
12. Nahid Shahabadi, Soheila Kashanian, Farivash Darabi, Euro. J. Med. Chem, 45 (2010) 4239.
13. Natarajan Raman, Narayanaperumal Pravin, Spectrochim. Acta Part A.118 (2014) 867.

14. M. Munakata, L.P. Wu, M. Yamamoto, T. Kuroda Sowa, M. Maekawa, S. Kawata, S. Kitagawa, J. Chem. Soc. Dalton Trans. 72 (1995) 4099.
15. A.B.P. Lever, Inorganic Electronic Spectroscopy, Elsevier, Amsterdam. (1984).
16. B.T. Hathway, Struct. Bonding. 14 (1973) 60.
17. R.C. Maurya, B. Shukla, J. Chourasia, S. Roy, P. Bohre, S. Sahu, M. H. Martin, Indian J. Chem. 47 (2008) 517.
18. M.J. Waring, in: G.C.K. Roberts (Ed.), Action at the Molecular Level, Macmillan. London (1977) 166.
19. K. Tsai, T.G. Hsu, K.M. Hsu, H. Cheng, T.Y. Liu, C.F. Hsu, C.W. Kong, Free Radic. Biol. Med. 31 (2001) 1465.
20. S. Sathiyaraj, K. Sampath, R.J. Butcher, R. Pallepogu , C. Jayabalakrishnan, Eur. J. Med. Chem. 64 (2013) 81.
21. N. Udilova, A.V. Kozlov, W. Bieberschulte, K. Frei, K. Ehrenberger, H. Nohl, Biochem. Pharm. 65 (2003) 59.
22. Charikleia Tolia, Athanassios N. Papadopoulos, Catherine P. Raptopoulou, Vassilis Psycharis, Claudio Garino, Luca Salassa, George Psomas. J. Inorg. Biochem. 123 (2013) 53.
23. M.A. Neelakantan, F. Rusalraj, J. Dharmaraj, S. Johnsonraja, T. Jeyakumar, M. Sankaranarayana Pillai, Spectrochim. Acta Part A. 71 (2008) 1599.
24. A.M. Pyle, T. Morri, J.K. Barton, J. Am. Chem. Soc. 112 (1990) 9432.
25. M.C. Prabahara, H.S. Bhojya Naik, Biometals. 21 (2008) 675.
26. Angamuthu Raja, Venugopal Rajendiran, Palanisamy Uma Maheswari, Ramalingam Balamurugan, Colin A. Kilner, Malcolm A. Halcrow and Mallayan Palaniandavar , J. Mol. Struct, 99 (2005) 1717.
27. Yong-Jun Zheng, Xiao-Wen Li, Yan-Tuan Li, Zhi-Yong Wub and Cui-Wei Yan, J of Photochem and Photobio B, 114 (2012) 27.
28. N. Raman, A. Selvan and P. Manisankar, Spectrochim. Acta Part A, 76 (2010) 161.
29. Farukh Arjmand, Fatima Sayeed and Mohd. Muddassir, J of Photochem and Photobio, 103 (2011) 166.

APPENDICES

Figure Captions

Figure 1: Schematic route for synthesis of Schiff base ligand and its metal complexes.

Figure 2: ^{1}H NMR spectrum of Schiff base ligand -1.

Figure 3: 3D structure of Cu($C_{42}H_{34}N_4O_6$) complex.

Figure 4: Agarose gel showing the results of electrophoresis of pBR322 DNA with the Schiff base complexes : Lane 1, pBR322 DNA - Control; Lane 2, DNA + H_2O_2 (1mM); Lane 3, DNA + H_2O_2 (1mM) + Co($C_{42}H_{34}N_4O_6$) (50µM); Lane 4, DNA + H_2O_2 (1mM) + Cu($C_{42}H_{34}N_4O_6$) (50µM) + H_2O_2; Lane 5, DNA + H_2O_2 (1mM) + Mn($C_{42}H_{34}N_4O_6$) (50µM) + H_2O_2; Lane 6, DNA + H_2O_2 (1mM) + Ni($C_{42}H_{34}N_4O_6$) (50µM).

Figure 5: Electronic absorption spectra of Cu($C_{42}H_{34}N_4O_6$) complex in the absence and presence of increasing amounts of DNA. Arrows show the absorbance changes upon increasing DNA concentration. (Complex in Tris-HCl buffer

upon addition of CT DNA).

Figure 6: Plots of [DNA]/ (ε_a-ε_f) versus [DNA] for the titration of Cu($C_{42}H_{34}N_4O_6$) with CT-DNA.

Figure 7: Effect of increasing amounts of EB (♦) and in the presence of increasing concentrations of $C_{20}H_{16}N_2O_4$ (●), $C_{22}H_{20}N_2O_2$ (■), and its Cu($C_{42}H_{34}N_4O_6$) (■), Ni($C_{42}H_{34}N_4O_6$) (▲), Co($C_{42}H_{34}N_4O_6$) (+), Mn($C_{42}H_{34}N_4O_6$) (X) on the relative viscosity of CT DNA at 30 °C. [DNA] = 1.5mM.

Table Captions

Table 1: Anti-biogram Assay of the Schiff Base and Its Mononuclear Metal Complexes

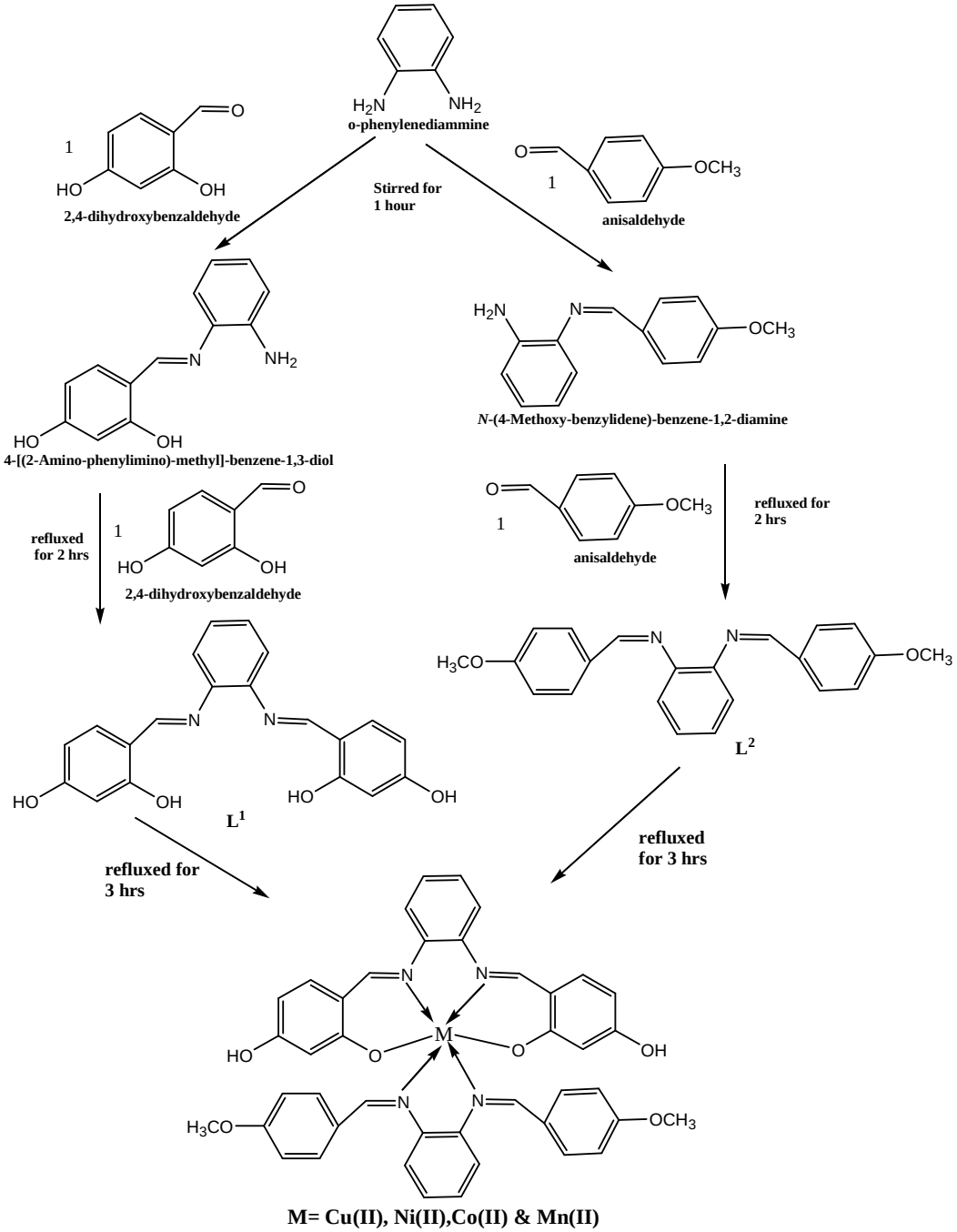

Figure 1

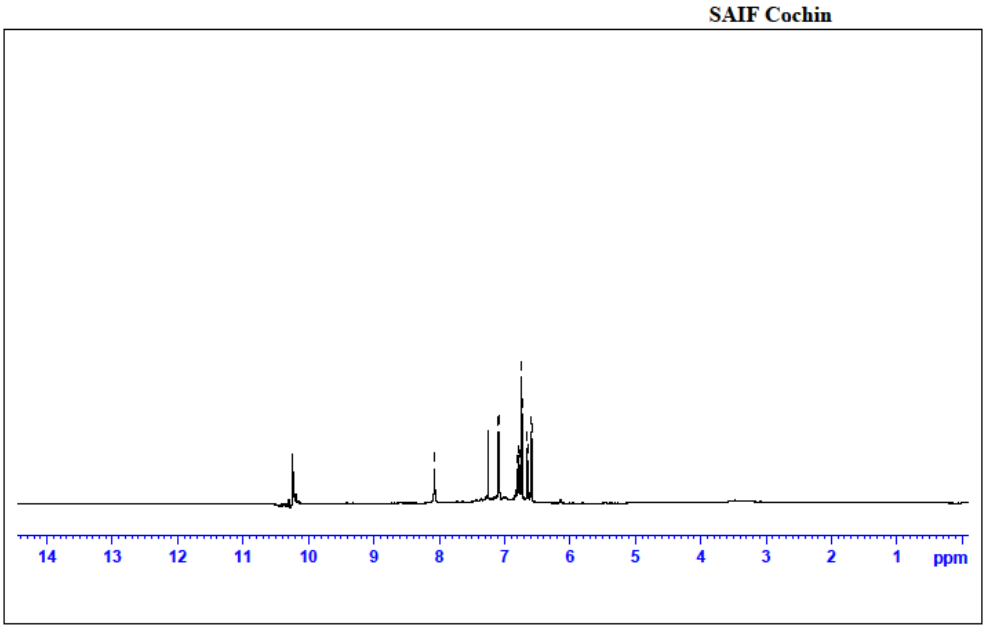

Figure 2

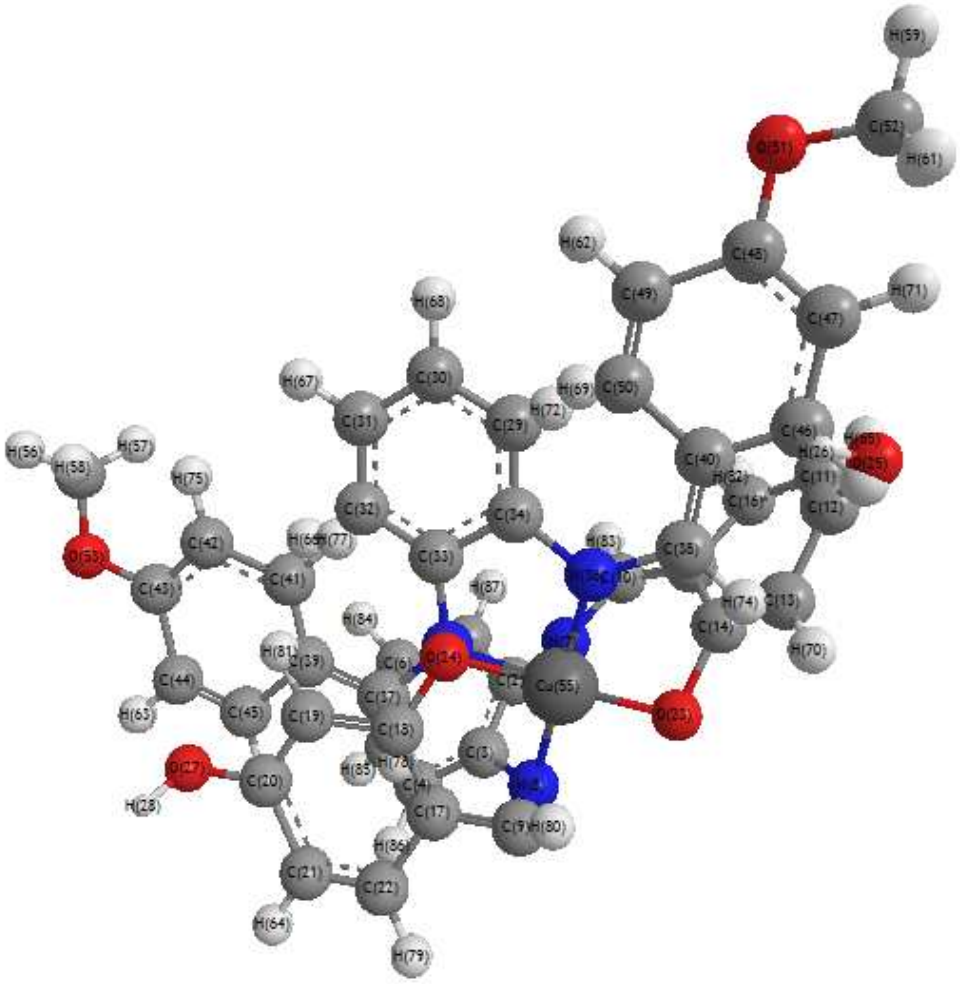

Figure 3

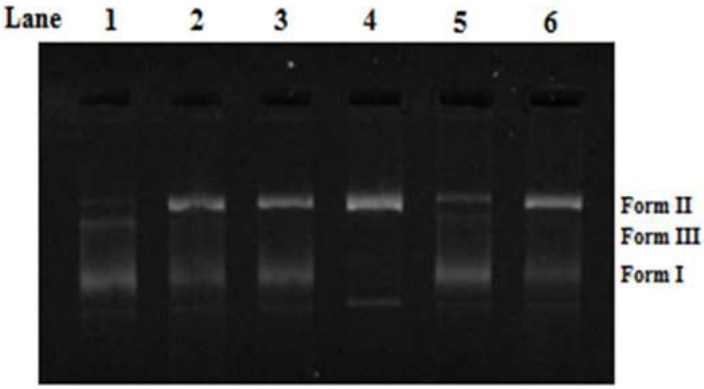

Figure 4

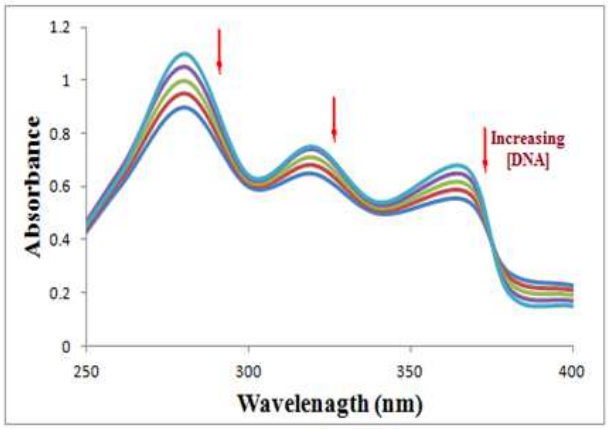

Figure 5

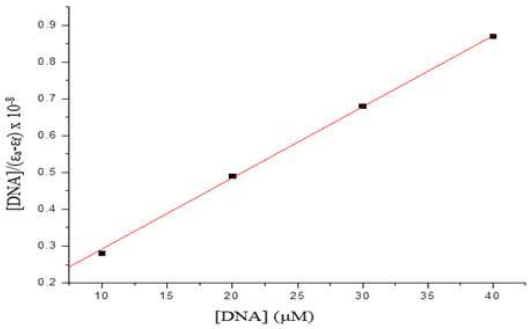

Figure 6

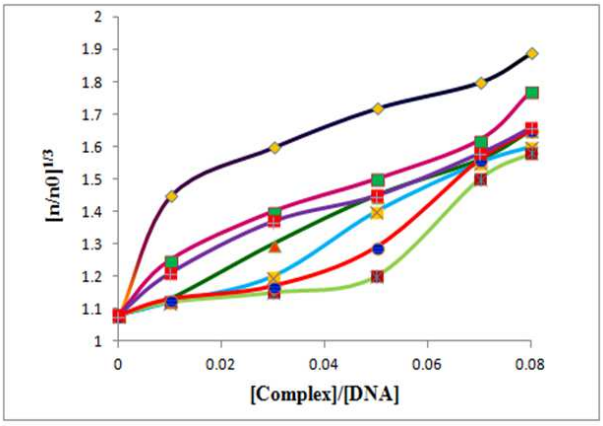

Figure 7

Table 1: Anti-Biogram Assay of the Schiff Base and Its Mononuclear Metal Complexes

Samples	Diameter of Inhibition Zone (Mm) [A] ; Concentration in µg/ Ml					
	% Activity Index					
	Gram-Positive Bacteria		Gram-Negative Bacteria		Fungi	
	S. aureus	*B. subtilis*	*K. pneumoniae*	*E. coli*	*F. oxysporum*	*A. fumigatus*
Streptomycin	24± 0.2	25± 0.4	25± 0.2	23± 0.2	-	-
Clotrimazole	-	-	-	-	21± 0.1	23± 0.2
$C_{20}H_{16}N_2O_4$	7± 0.3	8± 0.2	7± 0.3	6± 0.4	8± 0.3	7± 0.3
$C_{22}H_{20}N_2O_2$	6± 0.2	7± 0.1	7± 0.2	6± 0.3	6± 0.1	7± 0.1
$Cu(C_{42}H_{34}N_4O_6)$	17± 0.4	15± 0.3	16± 0.4	14± 0.1	18± 0.2	17± 0.1
$Ni(C_{42}H_{34}N_4O_6)$	12± 0.3	14± 0.2	13± 0.2	12± 0.1	16± 0.4	17.5± 0.2
$Co(C_{42}H_{34}N_4O_6)$	13± 0.2	15± 0.2	13± 0.5	12± 0.2	19± 0.2	20± 0.2
$Mn(C_{42}H_{34}N_4O_6)$	11± 0.5	13± 0.4	12± 0.4	10± 0.3	16± 0.3	15± 0.2

a Average of three replicates